Thin-Walled Structures 132 (2018) 596–603

Contents lists available at ScienceDirect

Thin-Walled Structures

journal homepage: www.elsevier.com/locate/tws

Full length article

Modal analysis of inflated membrane cone considering pressure follower force effect

Rui-Qiang Ma, Jian-Zheng Wei, Hui-Feng Tan*, Zhi-Han Yang

Centre for Composite Materials and Structures, Harbin Institute of Technology, Harbin 150080, China

ARTICLE INFO

Keywords:
Membrane structures
Inflated cone
Beam model
Modal analysis
Follower force effect

ABSTRACT

Inflated membrane cones have attracted extensive research efforts in various fields owing to features such as ultra-light weight, high packaging efficiency. The pressure effect was considered in the vibration analysis of these structures because pressure was the main contributor to structural stiffness. Based on the virtual work principle and Timoshenko beam theory, an improved beam model considering the pressure effect, which includes the prestress stiffness and follower force effects, was proposed for the vibration of an inflated cone. The results calculated from the proposed model agreed strongly with the experimental results. Moreover, the pressure follower force effect was investigated using different pressures and taper angles. The study proved that the follower force effect decreased the natural frequencies in lower modes, and increased them in higher modes.

1. Introduction

Owing to their ultra-light weight, great packaging package efficiency, and high deployment reliability, inflated membrane structures have extensive applications in aerospace [1–4] and civil engineering [5,6]. Numerous inflated structures, such as airships, inflated wings, and certain structural components, can be regarded as inflated cones [7]. The inflated cone vibration is easy to be affected by the inflated pressure caused by its low structural stiffness. Accurate modal analysis is the basis for evaluating the dynamic performance of such a structure [8].

Jha et al. [9] indicated that the pressure effect includes the prestress stiffness and follower force effect. The prestress stiffness effect refers to the change in the structure's load-bearing as a result of the prestress field induced by the pressure. The follower force effect occurs because the pressure tends to be perpendicular to the deflected surface, and this deflection-dependent force can change the effective stiffness of the inflated structure. The effects of stiffness effects on the vibration characteristics of the plate, shell and membrane structure were studied in [10–14]. Several analysis models for the prestress stiffness effect have been proposed, including the hexagonal membrane element model [13] and nine-node membrane element model [14]. Hu et al. [8] conducted a numerical analysis of membrane structures considering the pre-stress effect, and indicated that the follower force effect should be considered in the membrane element stiffness matrix. To improve the accuracy of inflated membrane structures, several shell and membrane models considering the follower force effect have been established [9,15–17]. Liu and He [18] compared the natural frequency of an inflated torus with and without the pressure follower force effect, and concluded that the natural frequency could be reduced by approximately 25–60% as a result of the follower force effect.

Alternatively, the beam model can provide a more efficient solution for large space structures consisting of inflated cones, beams and tori than the shell and membrane model. Thomas and Wielgosz [19] had established an inflated beam theory that takes into account the geometrical stiffness and follower forces effect for the deflection of the inflated tube. In the bending and buckling analysis of inflated beams, a beam element considering the pressure effect was proposed in the literature [20,21]. Thomas et al. [22] and Apedo et al. [23] developed a dynamic stiffness matrix related to the natural frequency and inflation pressure of an inflated beam.

Inflated beams with constant sections have been studied extensively, but not as much research has been conducted on inflated cones with variable section. This study proposed an improved beam model aimed at an inflated cone. The test and membrane models were implemented to verify the proposed beam model (PBM). Following this, the influences of the follower force effect on the modal characteristics were studied, and the deviation of the test and PBM was researched. The results demonstrated that the follower force effect had a substantial influence on the first five bending modal frequencies, and it was significantly greater than the gas effect on the natural frequency at a high pressure. The lower natural frequencies were fairly reduced because of

* Corresponding author.
E-mail address: tanhf@hit.edu.cn (H.-F. Tan).

https://doi.org/10.1016/j.tws.2018.09.007
Received 8 March 2018; Received in revised form 29 August 2018; Accepted 2 September 2018

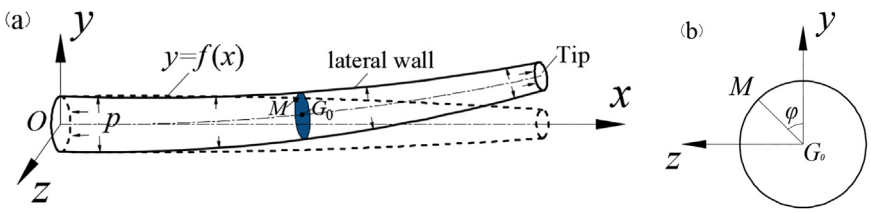

Fig. 1. Model of inflated cantilever cone: (a) inflated cone and (b) cross-section.

the consideration of the follower force effect, while the higher natural frequencies increased by a small amount.

2. Numerical model

This section is based on the Timoshenko beam theory, and the beam model of the inflated cone after moulding is established here. Fig. 1 illustrates a cantilever inflated cone model, which has the generatrix equation $y = f(x)$. The xyz represented the Cartesian coordinates, and the x-axis indicated the axis direction of the inflated cone; with the coordinate origin O located at the dot of the fixed end. To make the theoretical model concise and easy to understand, this study made the following assumptions:

(1) The cross-section of the inflated cone remained flat during the vibration deformation;
(2) The initial axial internal force was constant, while the initial bending moment and shear stress were zero; and
(3) The ratios of the y-direction displacement to the length and cross-section rotation were the first-order small quantities, while the ratio of the x-direction displacement to the length was a second-order small quantity.

Based on the first assumption, the displacement vector $\mathbf{U}$ can be expressed as,

$$\mathbf{U} = \begin{cases} u - y\sin\theta \\ v - y(1 - \cos\theta) \\ w \end{cases} \tag{1}$$

where u, v and w were the x, y and z-direction displacements of the central point of the cross-section including point M, respectively; and θ was the cross-section rotation around the z-axis. As the bending mode in the xy and xz planes was identical, the 2D beam model was studied in the xy plane. Thus, w was considered to be zero. The virtual displacement of point M was obtained by the variation of Eq. (1):

$$\delta\mathbf{U} = \begin{cases} \delta u - y\cos\theta\cdot\delta\theta \\ \delta v - y\sin\theta\cdot\delta\theta \\ 0 \end{cases} \tag{2}$$

The Green–Lagrange strain $\mathbf{E}$ of the inflated cone can be expressed as,

$$\mathbf{E} = \frac{1}{2}[\nabla\mathbf{U} + \nabla^{\mathrm{T}}\mathbf{U} + \nabla^{\mathrm{T}}\mathbf{U}\cdot\nabla\mathbf{U}] \tag{3}$$

where $\nabla\mathbf{U}$ denoted the gradient of $\mathbf{U}$ and $\nabla^{\mathrm{T}}\mathbf{U}$ is its transpose tensor.

2.1. Dynamic equilibrium equation

The virtual work principle was applied to establish the dynamic equilibrium equation of the inflated cone. The virtual work equation is

$$\delta W_{acc} + \delta W_{int} + \delta W_{ext} = 0 \tag{4}$$

where δW_{acc}, δW_{int} and δW_{ext} denote the virtual work of the inertia, internal and external forces, respectively.

2.1.1. Virtual work of inflated pressure

The virtual work of the inflated pressure in the inflated cone was analysed. The inflated pressure following moulding was stable in this study, the pressure was considered as uniform. Moreover, based on the third assumption, the pressure was approximated as a constant in the vibration deformation. Unlike shell and membrane models, the inflated pressure at the inflated cone wall cannot be applied directly in the beam model. Therefore, the inflated pressure was introduced into the structural stiffness matrix as an influence factor. The virtual work of the inflated pressure on the inflated cone's lateral wall and tip was then examined. The coordinates of the arbitrary point M(x,y,z) in the lateral wall can be expressed as

$$\begin{cases} x = x \\ y = f(x)\cdot\cos\varphi \\ z = f(x)\cdot\sin\varphi \end{cases} \tag{5}$$

where φ was the angle of the line G_0M and the y-axis (Fig. 1(b)), and x was the axial coordination. Based on Eq. (5), the following equation was obtained:

$$\mathbf{n}ds = -f(x)\begin{bmatrix} v_{,x}\cos\varphi + f'(x)\cos\theta - f(x)\cos^2\varphi.\ \sin\theta\cdot\theta_{,x} \\ f'(x)\sin\theta - \cos\varphi\cdot(1 + u_{,x} - \cos\varphi\cos\theta\cdot\theta_{,x}) \\ -\sin\theta\cdot(\cos\theta + u_{,x}\cos\theta + v_{,x}\cdot\sin\theta - f(x)\cos\varphi\cdot\theta_{,x}) \end{bmatrix} dxd\varphi \tag{6}$$

where, $\mathbf{n}$ was the normal vector of the inflated cone wall and ds was the element area. Thus, the virtual work of the inflated pressure on the lateral wall was represented as

$$\begin{aligned} \int_{\mathrm{lat}} p\cdot\delta\mathbf{U}\cdot\mathbf{n}ds &= -p\pi\cdot\int_0^l f(x)[(2f'(x)\cdot\cos\theta - f(x)\sin\theta\cdot\theta_{,x})\delta u \\ &+ (2f'(x)\cdot\sin\theta + f(x)\cdot\cos\theta\cdot\theta_{,x})\delta v \\ &- (f(x)\cdot\cos\theta\cdot v_{,x} - f(x)\sin\theta(1 + u_{,x}))\delta\theta]dx \end{aligned} \tag{7}$$

where p was the inflated pressure in the inflated cone and the integration area "lat" was the inner surface of the lateral wall. Similarly, the virtual work of the inflated pressure on the tip was denoted as

$$\int_{\mathrm{tip}} p\cdot\delta\mathbf{U}\cdot\mathbf{n}ds = p\pi f^2(l)\cdot(\cos\theta\cdot\delta u + \sin\theta\cdot\delta v)_{x=l} \tag{8}$$

where, the integration area 'tip' was the inner surface of the tip.

2.1.2. Virtual work of internal force

The virtual work of the internal force was analysed in this section. Based on Eq. (3), the component items E_{xx}, E_{xy} and E_{yy} of the Green-Lagrange strain $\mathbf{E}$ were obtained, respectively:

$$E_{xx} = u_{,x} - y\cos\theta\cdot\theta_{,x} + \frac{1}{2}[(u_{,x})^2 + (v_{,x})^2 + (y\theta_{,x})^2] - y\cos\theta \cdot u_{,x}\theta_{,x} - y\sin\theta\cdot v_{,x}\theta_{,x} \tag{9a}$$

$$E_{xy} = \frac{1}{2}[v_{,x} - (1 + u_{,x})\sin\theta] \tag{9b}$$

$$E_{yy} = 0 \tag{9c}$$

Therefore, the virtual strains were

$$\begin{aligned} \delta E_{xx} &= (1 + u_{,x} - y\cos\theta\cdot\theta_{,x})\delta u_{,x} + [y^2\theta_{,x} - y\cos\theta(1 + u_{,x}) \\ &- y\sin\theta\cdot v_{,x}]\delta\theta_{,x} + (v_{,x} - y\sin\theta\cdot\theta_{,x})\delta v_{,x} \\ &+ [y\sin\theta\cdot\theta_{,x}\cdot(1 + u_{,x}) - y\cos\theta\cdot\theta_{,x}v_{,x}]\delta\theta \end{aligned} \tag{10a}$$